

MULTI-POINT DESIGN OF A SUPERSONIC WING USING MODIFIED PAR-SEC AIRFOIL REPRESENTATION

T. Yotsuya¹, M. Kanazaki², Y. Makino³, and K.Matsushima⁴

¹ Graduate School of System Design, Department of Aerospace Engineering, Tokyo Metropolitan University (kana@sd.tmu.ac.jp)

² Faculty of System Design, Division of Aerospace Engineering, Tokyo Metropolitan University

³ Aviation Program Group, Japan Aerospace Exploration Agency (JAXA)

⁴ Faculty of Engineering, University of Toyama

Abstract. *This paper discusses the multi-point aerodynamic design of a supersonic wing. Herein, supersonic transport (SST) which cruises over land at a low Mach number (around $M = 1.15$) and cruises over sea at a high Mach number (around $M = 2.0$). No sonic boom is said to be heard on the ground because of the “Mach cutoff effect.” This concept requires that high aerodynamic performance should be achieved at a high and a low Mach number cruise, simultaneously. Thus, this study considers a multi-point design aerodynamic problem. The objective functions considered here are employed to maximize the lift-to-drag ratio at cruise speed $M=1.15$, and $M=2.0$, simultaneously. Thus, the several flow conditions should be considered. To solve such multi-objective design problem, efficient global optimization (EGO) was applied. The EGO process is based on Kriging surrogate models, which were constructed using several sample designs. Subsequently, the solution space could be explored through the maximization of expected improvement (EI) values that corresponded to the objective function of each Kriging model because the surrogate models provide an estimate of the uncertainty at the predicted point. Once a number of solutions have been obtained for the EI maximization problem by means of a multi-objective genetic algorithm (MOGA), the sample designs could be used to improve the models’ accuracy and identify the optimum solutions at the same time. In this paper, 193 sample points are evaluated for the constructions of the Kriging model, and several design are compared. Remarkably, the kink airfoil should be similar to typical subsonic airfoil to achieve higher aerodynamic performance not only at high speed cruise but also low speed cruise in spite of supersonic cruise.*

Keywords: *Modified PARSEC Representation, Efficient Global Optimization, Mach Cutoff Effect.*

1. INTRODUCTION

There are many studies on the reduction of the sonic boom intensity. One idea to reduce the sonic boom is flying at lower Mach number on the ground. No sonic boom is said to be heard on the ground because of the “Mach cutoff effect.” In fact, Aerion’s SBJ [1] cruises over land at a low Mach number (around $M = 1.15$) and cruises over sea at a high Mach number (around $M = 1.60$). This concept requires that high aerodynamic performance be achieved at a high as well as a low Mach number cruise. Thus, a multi-point design needs to be considered.

The goal of this work is the multi-point aerodynamic design of a supersonic wing by means of the high efficient and global wing design methodology, which includes Kriging based multi-objective genetic algorithm (MOGA) [2], and the modified PARAmetric SEction (PARSEC) airfoil representation [3]. This study considers the design problem which has two objective functions, which are the minimization of the drag coefficient (C_D) at the Mach numbers of 1.15 and 2.0, simultaneously. Obtained designs are compared with the reference design (baseline) which was designed based on the Carlson’s warp theory for the Japanese experimental model, NEXST-1 by Japan Aerospace Exploration Agency (JAXA).

In addition, this study considers the minimization of the difference of the moment coefficient ($|C_M|$) between the baseline and the designed wing. Conventionally, aircraft’s wing design has been considered that the lift by the wing equal to the aircraft weight. In such design, trim balance by the horizontal tail should be considered after the wing is designed, and the drag by the horizontal tail is not always minimized. As this result, there is possibility of increasing the total drag, even if the drag of the main wing has been minimized. With these facts, this study considers the minimization of $|C_M|$. $|C_M|$ is evaluated at $M=2.0$, because the baseline wing is designed in consideration of the drag minimization at $M=2.0$.

In this study, wing cross sectional geometries are designed according to the modified PARSEC airfoil representation [3] proposed in our previous study. The wing planform remains the same as the wing of NEXST-1. The aerodynamic performance is evaluated by means of computer-aided design (CAD)-based automatic panel analysis (CAPAS) developed at JAXA [4, 5].

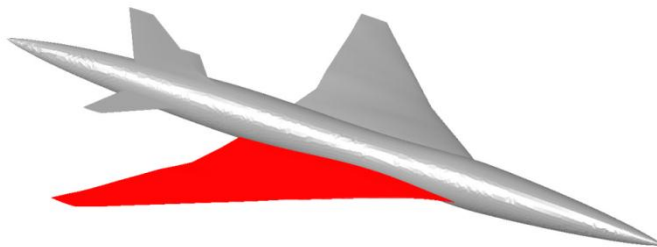


Figure 1. Geometry of NEXST-1. The wing colored by red is baseline design in this study.

2. WING DESIGN METHOD

The original PARSEC airfoil representation is a generic design method for a conventional transonic airfoil by Professor Sobieczky [6]. In this method, geometric parameters for the airfoil's suction side and pressure side are separately defined based on the aerodynamic theory of transonic flow (Fig. 2). Using the original PARSEC representation, super-critical airfoils can be designed with a detailed camber design around the trailing edge to control the local shock on the upper surface. However, because it has a number of design parameters around the leading edge, it is difficult to apply this airfoil design in supersonic flows. Modification of the original PARSEC representation was proposed [3], and the existing supersonic/transonic airfoil was represented very well. This method defines the airfoil's thickness and camber, separately. This idea is based on the common theory of a wing section, as shown in Fig. 3(a). The thickness distribution and the camber are defined by Eqs. (1) and (2), respectively. Eq. (1) corresponds to a symmetrical airfoil using the original PARSEC method, while the camber is defined by a quintic equation. A square root term is added to this equation as shown Eq. (2). By weighting this term (Fig. 3(b)), the camber of the leading edge can change independently. This modification is expected to represent an airfoil with a drooping leading edge.

$$z = \sum_{n=1}^6 a_n \times x^{\frac{2n-1}{2}} \quad (1)$$

$$z = b_0 \times \sqrt{x} + \sum_{n=1}^5 b_n \times x^n \quad (2)$$

The a_n and b_n values are determined from 11 parameters in this modification, as shown in Fig. 2.

In this study, the airfoil geometry at wing root, kink and tip are defined based on Eqs. (1) and (2). The wing planform is fixed as NEXST-1 as shown in table 1. The parameters of modified PARSEC representations are distributed along the wing span based on the polynomial as expressed as below.

$$dv_i = \sum_{v=0}^N \rho_v \cdot z^v \quad (3)$$

dv_i are values of design variables by modified PARSEC representation. A cross section i is interpolated by dv_i . ρ_v is calculated using three airfoils, the wing root, the kink, the tip, and two cross sections (CS1, 2) which is in the middle of the inboard wing and the outboard wing as shown in Fig. 4.

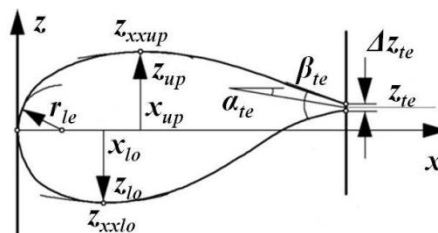


Figure 2. original PARSEC method [6].

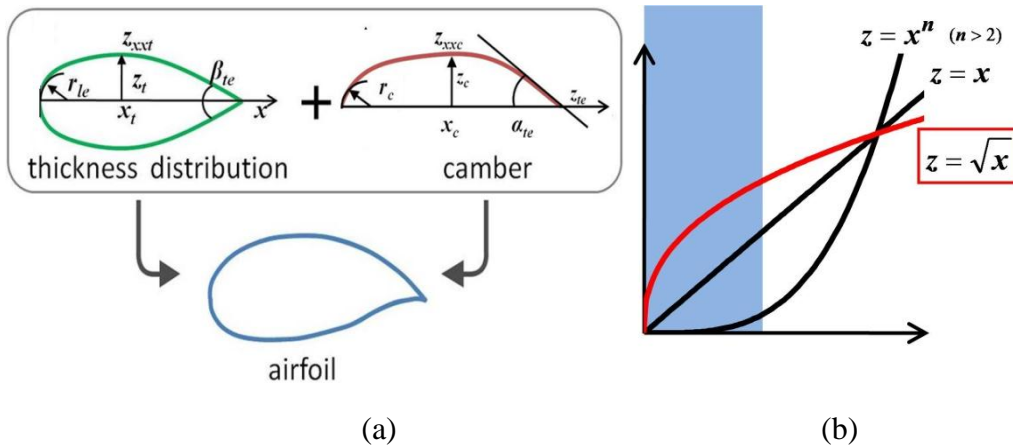


Figure 3. Definition of the airfoil by means of modified PARSEC method [3]

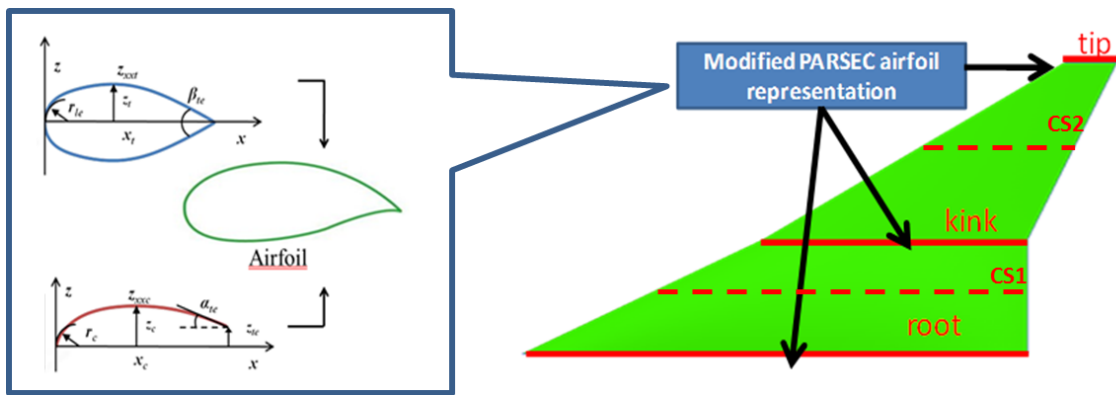


Figure 4. Planform geometry and cross sections to be designed.

Table 1. Planform parameters

Wing area	10.12 m ²
Span length	4.718
Aspect ratio	2.20
Taper ratio (inboard)	0.52
Taper ratio (outboard)	0.20
Sweep back angle (inboard)	66.0 deg.
Sweep back angle (outboard)	61.2 deg.
MAC length	2.754 m

3. DESIGN EXPLORATION METHODS

The optimization procedure followed for the design of the super sonic wing consists of the following steps (see Fig. 5). First, N design samples are selected by means of Latin hypercube sampling (LHS) [2] which is a space filling method and then assessed for the construction of a Kriging surrogate model. Second, n additional design samples are added and the design's accuracy is improved by constructing a new Kriging model based on all $N+n$ samples. It should be noted that the n additional samples are selected using expected

improvement (EI) maximization [2]. Furthermore, MOGA is applied to solve this maximization problem. This process is iterated until the improvement of the objective functions becomes negligible. Finally, the non-dominated front is examined, while data mining techniques are applied to obtain the further information about the design problem. EI values have been introduced as a selection criterion. The EI values for the minimization problem as:

$$EI(x) = (f_{\min} - \hat{y})\Phi\left(\frac{f_{\min} - \hat{y}}{s}\right) + s\phi\left(\frac{f_{\min} - \hat{y}}{s}\right) \quad (4)$$

where f_{\min} is the minimum value among all the available sample points and \hat{y} is the predicted value by Kriging model at an unknown point x . On the other hand, Φ and ϕ are the standard distribution and normal density, respectively.

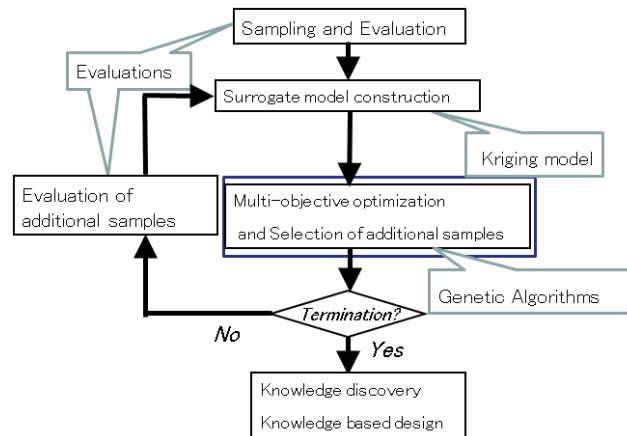


Figure 5. Procedure for the efficient exploration of the global design model

4. FORMULATIONS

4.1. Design Variables

Parameterization of the supersonic wing is expressed as Section 2. This study assumes that the wing tip has no camber (symmetrical airfoil) which has possibility to achieve low induced drag. At the wing kink and the wing tip, wash out angles are defined. The design variables and their range are summarized in Table 2. In this study, thickness of the wing is fixed to same values as NEXST-1 (root $0.043c$, kink $0.033c$, and tip $0.033c$).

Table 2 Design variables and their values

Design variables			lower	Upper
r_{le}	root	$dv1$	0.0001	0.0010
	kink	$dv2$	0.0001	0.0010
	tip	$dv3$	0.0001	0.0010
x_t	root	$dv4$	0.40	0.55
	kink	$dv5$	0.40	0.55
	tip	$dv6$	0.30	0.50
z_{xt}	root	$dv7$	-0.30	0.00
	kink	$dv8$	-0.20	0.00
	tip	$dv9$	-0.20	0.00
β_{te}	root	$dv10$	0.00	6.00
	kink	$dv11$	0.00	5.00
	tip	$dv12$	0.00	5.00
r_c	root	$dv13$	0.000	0.001
	kink	$dv14$	0.000	0.001
x_c	root	$dv15$	0.20	0.50
	kink	$dv16$	0.20	0.50
z_c	root	$dv17$	0.000	0.020
	kink	$dv18$	0.000	0.008
z_{xc}	root	$dv19$	-0.20	0.00
	kink	$dv20$	-0.20	0.00
z_{te}	root	$dv21$	-0.01	0.01
	kink	$dv22$	-0.01	0.01
α_{te}	root	$dv23$	-5.00	1.00
	kink	$dv24$	-2.00	2.00
wash out angle	kink	$dv25$	-2.00	4.00
	tip	$dv26$	0.00	6.00

4.2. Objective functions

The objective functions are derived through the simultaneous minimization of C_D at Mach 2.00, and 1.15. Each C_D value is evaluated at a target $C_L = 0.107$ at Mach 2.00 (an altitude of 19,000m) and $C_L = 0.108$ at Mach 1.15 (an altitude of 12,000m). Additionally, the difference of the moment coefficient between the designed wing and the NEXST-1 wing, $|\Delta C_M| (=|C_M - C_{M, NEXST1}|)$, is also an objective function to be minimized. The increment of the trim drag can be suppressed with $|\Delta C_M|$ minimization, because the aerodynamic performance of NEXST-1 is optimized at Mach 2.00. In other words, $|\Delta C_M|$ should be zero to achieve same level C_M as NEXST-1 at Mach 2.00. The aerodynamic performance is evaluated by means of CAPAS, as shown in Fig. 6. CAPAS includes the CATIA® v4/v5 application programming interface (API) and a full potential solver combined with a panel method [4, 5].

To obtain the additional sample designs described in Section 3, three EI values are simultaneously maximized by means of MOGA. On the other hand, the EI values are calculated based on three different Kriging models; $EI_{CD, M=2.00}$ and $EI_{CD, M=1.15}$, and $EI_{|\Delta C_M|}$. Eq. (4) is written for the present design problem as

$$\left\{ \begin{array}{l} \text{Minimizing} \\ \text{Minimizing} \\ \text{Minimizing} \end{array} \right. \begin{array}{l} EI_{CD, M=2.00} = (C_{D, M=2.00} - \hat{y}) \Phi \left(\frac{C_{D, M=2.00 \min} - \hat{y}}{s} \right) + s \phi \left(\frac{C_{D, M=2.00 \min} - \hat{y}}{s} \right) \\ EI_{CD, M=1.15} = (C_{D, M=1.15} - \hat{y}) \Phi \left(\frac{C_{D, M=1.15 \min} - \hat{y}}{s} \right) + s \phi \left(\frac{C_{D, M=1.15 \min} - \hat{y}}{s} \right) \\ EI_{|\Delta C_M|} = (|\Delta C_M| - \hat{y}) \Phi \left(\frac{|\Delta C_M|_{\min} - \hat{y}}{s} \right) + s \phi \left(\frac{|\Delta C_M|_{\min} - \hat{y}}{s} \right) \end{array} \quad (8)$$

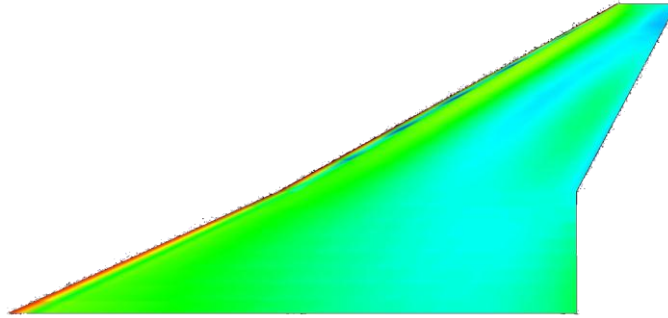


Figure 6. Pressure distribution along the aircraft surface estimated by means of CAPAS

5. DESIGN RESULTS

4.1. Sampling results

The results of the EGO process are shown in Fig. 7. In this study, EGO process was iterated three times, and total of 100 additional sample designs were obtained. Many additional samples could be added around the direction of the multi-objective optimum (non-dominated solutions, or approximate Pareto optimal set). This results suggests that the present design procedure could explore the design space very well. To compare the most promising samples for each objective function, three samples named DesA-B are evaluated.

4.2. Comparison of designed wing

Figure 8(a)-(d) shows the comparison of the airfoil geometry DesA-C, and NEXST-1. In the case of DesA, the lowest C_D at $M=2.00$ was achieved, DesB was one of the compromised solutionw. DesC was characterized by the lowest C_D at $M=1.15$. The value of the corresponding objective functions are summarized in Table 2. Comparing Fig. 8(a)-(c), the root airfoil and the tip airfoil of DesA-C are similar. Comparing with NEXST-1 as shown in Fig. 8(d), the tip airfoil of NEXST-1 is almost same as DesA-C. Additionally, the DesA-C and NEXST-1 have negative camber at the trailing edge of the root airfoil. Therefore, the design of the kink airfoil should decide the difference of the airodynamic performance should

dominated by the difference. The leading edge design of the root airfoil should similarly affect to the aerodynamic performance.

Comparing Fig. 8(a)-(d), DesA-C has negative camber at the root airfoil while NEXST-1 has positive camber. Therefore, DesA-C achieves lower C_D than NEXST-1 at $M=2.00$. According to Fig. 8(c), the airfoil at kink is similar to the typical transonic airfoil which has positive camber around trailing edge. As this result, the aerodynamic performance of DesC at lower Mach number is highest among the resulting samples.

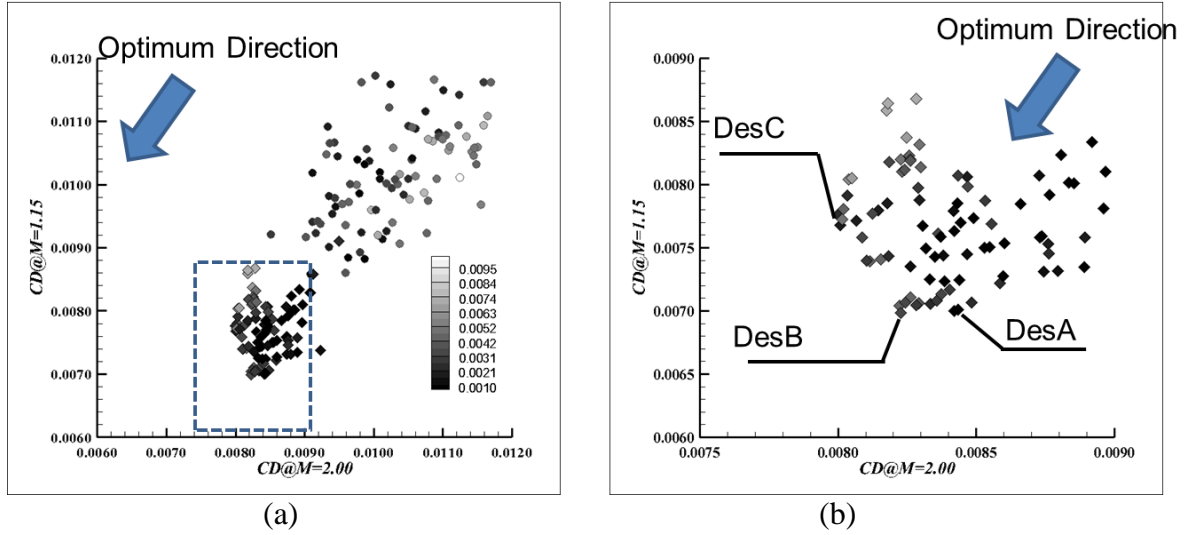
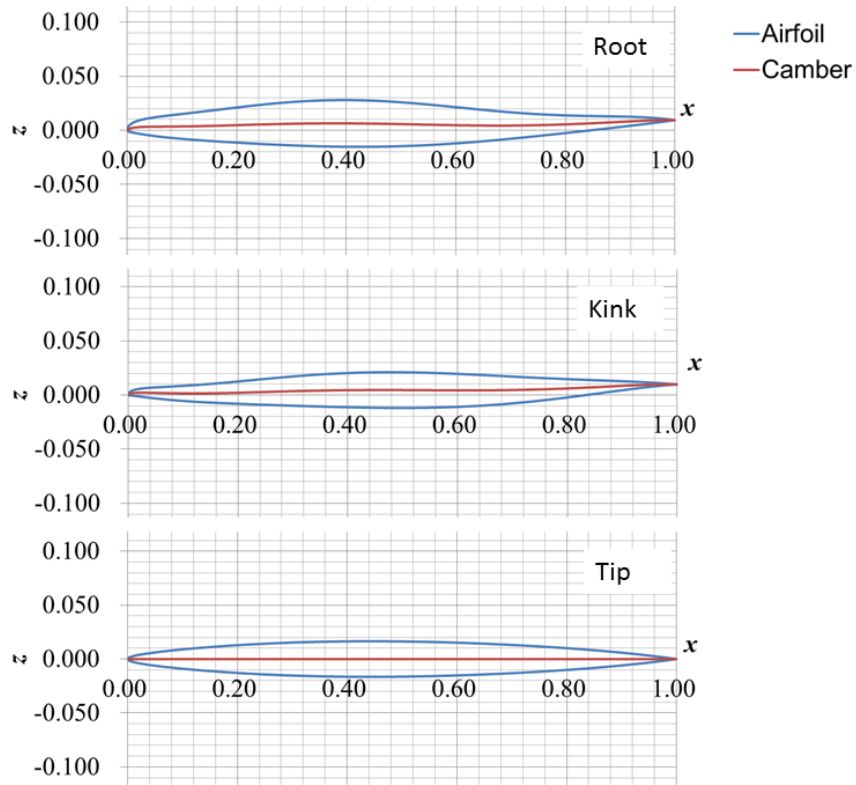


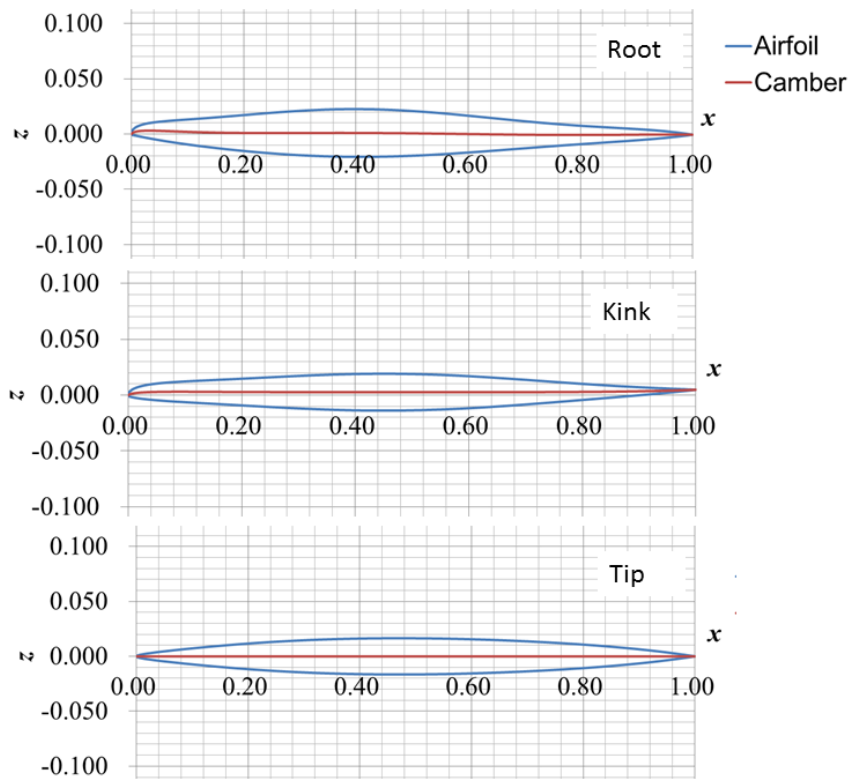
Figure 7. Sampling result by means of EGO, (a)all solutions, and (b)close up view around non-dominated solutions.

Table 2. Summary of the aerodynamic performance of the selected designs.

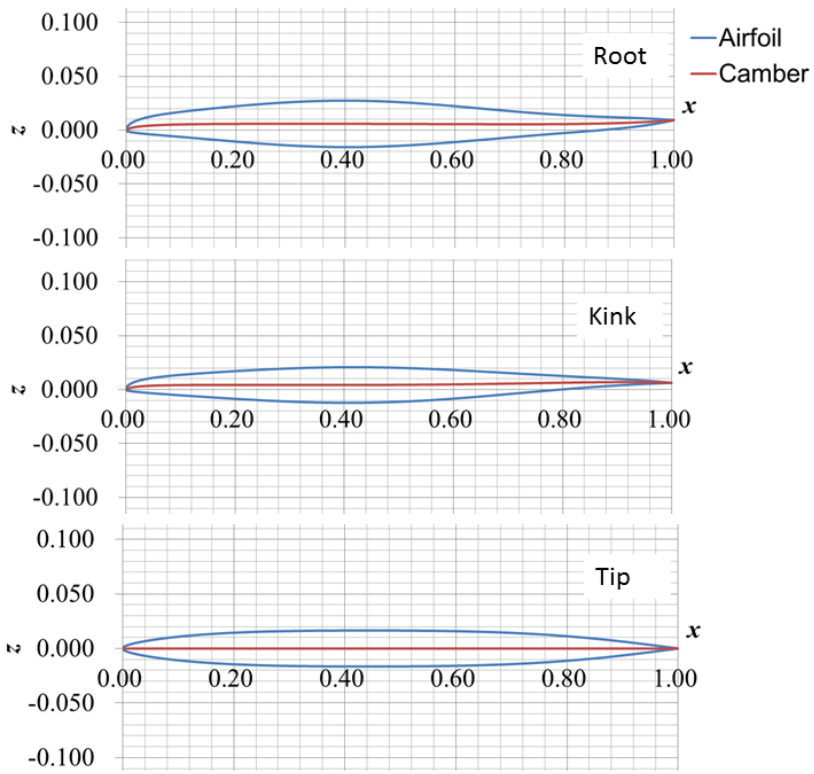
		C_D	$ \Delta CM $
DesA	M=2.00	0.00800	0.00249
	M=1.15	0.00776	0.00562
DesB	M=2.00	0.00810	0.00304
	M=1.15	0.00740	0.00409
DesC	M=2.00	0.00830	0.00326
	M=1.15	0.00699	0.00171
Baseline	M=2.00	0.09598	0.00000
	M=1.15	0.09019	0.00000



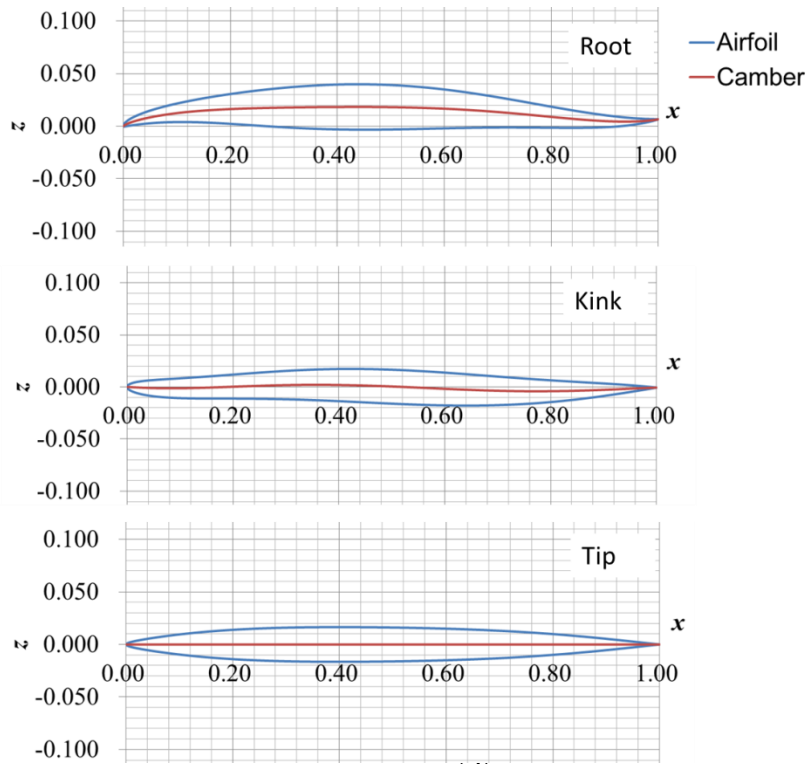
(a)



(b)



(c)



(d)

Figure 8. Comparison of the designed airfoil among DesA-C, and NEXST-1. (a)DesA, (b)DesB, (c)DesC, (d)NEXST-1.

5. REFERENCES

- [1] <http://aerioncorp.com/>
- [2] Jeong, S., Murayama, M., and Yamamoto, K., Efficient Optimization Design Method Using Kriging Model, *Journal of Aircraft*, Vol. 42, No.2 (2005), pp.413-420.
- [3] Matsuzawa, T., K. Matsushima, and Nakahashi, K., "Application of PARSEC Geometry Representation to High-Fidelity Aircraft Design by CFD," CD proceedings of 5th WCCM/ ECCOMAS2008, Venice, CAS1.8-4 (MS106), 2008.
- [4] Makino, Y., Low sonic-boom design of a Silent Super Sonic Technology Demonstrator ~ Development of CAPAS and its Application ~, JAXA Special Publication, Proceedings of International Workshops on Numerical Simulation Technology for Design of Next Generation Supersonic Civil Transport (2007), pp. 697-704.
- [5] Chiba, K., Makino, Y., and Takatoya, T., Design-Informatics Approach for Intimate Configuration of Silent Supersonic Technology Demonstrator, AIAA-2009-968, (2009).
- [6] Sobieczky, H., "Parametric Airfoils and Wings," Notes on Numerical Fluid Mechanics, pp. 71-88, Vieweg 1998.